cosmetics

MDPI

Article

In Vitro Hair Dermal Papilla Cells Induction by *Fagraea berteroana*, a Tree of the Marquesan Cosmetopoeia (French Polynesia)

Kristelle Hughes [1], Raimana Ho [1], Claire Chazaud [2], Stéphanie Hermitte [3], Stéphane Greff [4], Jean-François Butaud [5], Edith Filaire [3,6], Edwige Ranouille [3], Jean-Yves Berthon [3] and Phila Raharivelomanana [1,*]

1 UMR EIO 241, IFREMER, ILM, IRD, Université de la Polynésie Française, BP 6570, 98702 Faaa, Tahiti, French Polynesia; kristelle.hughes@doctorant.upf.pf (K.H.); raimana.ho@upf.pf (R.H.)
2 GReD Institute, Université Clermont Auvergne, CNRS, Inserm, Faculté de Médecine, CRBC, 63000 Clermont-Ferrand, France; claire.chazaud@uca.fr
3 Greentech SA, Biopôle Clermont-Limagne, 63360 Saint-Beauzire, France; stephaniehermitte@greentech.fr (S.H.); edithfilaire@greentech.fr (E.F.); developpement@greentech.fr (E.R.); jeanyvesberthon@greentech.fr (J.-Y.B.)
4 Institut Méditerranéen de Biodiversité et d'Ecologie Marine et Continentale (IMBE), UMR 7263 CNRS, IRD, Aix Marseille Université, Avignon Université, Station Marine d'Endoume, rue de la Batterie des Lions, 13007 Marseille, France; stephane.greff@imbe.fr
5 Consultant in Forestry and Polynesian Botany, BP 52832, 98716 Pirae, Tahiti, French Polynesia; jfbutaud@hotmail.com
6 UMR 1019 INRA-UcA, UNH (Human Nutrition Unity), ECREIN Team, Université Clermont Auvergne, 63000 Clermont-Ferrand, France
* Correspondence: phila.raharivelomanana@upf.pf

Citation: Hughes, K.; Ho, R.; Chazaud, C.; Hermitte, S.; Greff, S.; Butaud, J.-F.; Filaire, E.; Ranouille, E.; Berthon, J.-Y.; Raharivelomanana, P. *In Vitro* Hair Dermal Papilla Cells Induction by *Fagraea berteroana*, a Tree of the Marquesan Cosmetopoeia (French Polynesia). *Cosmetics* **2021**, *8*, 13. https://doi.org/10.3390/cosmetics8010013

Received: 14 December 2020
Accepted: 28 January 2021
Published: 4 February 2021

Abstract: *Fagraea berteroana* is a tree used in traditional medicine in various islands of the South Pacific. Here, we studied its hair growth-inducing properties as suggested by one of its Marquesan ethno-uses in haircare. The ethyl acetate extract of the fruits of *F. berteroana* (FEAE) and four resulting fractions (FEAE-F0, FEAE-F1, FEAE-F2, and FEAE-F3) were tested on hair follicle dermal papilla cells to determine their cell proliferative activity. Furthermore, RT-qPCR analysis enabled gene modulation analysis, while immunostaining of the β-catenin protein was used to follow protein regulation. We found that the plant extracts induced a controlled, dose-dependent cell proliferation. FEAE-F0 simultaneously down-regulated Bone Morphogenetic Protein 2 (*BMP2*) mRNA expression and upregulated Cyclin-D1 (*CCND1*) gene expression, which suggests an involvement in the regulation of the Wnt and Transforming Growth Factor beta (TGFβ) pathways that control the hair cycle. FEAE-F0 exhibited a 1.34-fold increase of nuclear β-catenin protein. This is indicative of an active hair growth state. Thus, we conclude that FEAE-F0 could be an innovative candidate in hair care, which opens interesting leads to promote the Marquesan cosmetopoeia.

Keywords: *Fagraea berteroana*; hair growth; ethnocosmetology; Marquesas islands; Gentianaceae

1. Introduction

Overall body care is an essential routine in Polynesian customs, as depicted by the confection and daily use of monoi and other natural preparations for embellishment [1–3]. Moreover, hair is an important physical feature in French Polynesia's society; it is the second most cited application area of cosmetics after the skin, in the Marquesas Islands [3]. As such, the imagery of Polynesians with long, luxurious, and silky dark hair is widespread, even to this day (Figure 1, [4,5]).

Figure 1. Left: Tahitian woman with hibiscus flower and waist-length hair. Credit: T. Theophilus, 2021. Center-left: White and yellow *Fagraea berteroana* flowers. Credit: J.-F. Butaud, 2005. Center-right: Unripe fruits of *F. berteroana* and white flower. Credit: K. Hughes, 2018. Right: Ripe *F. berteroana* fruit. Credit J.-F. Butaud, 2010.

An effort to study French Polynesia's cosmetopoeia [6] led to discovering one plant with an atypical traditional application. This scarcely known ethnocosmetic use was recorded in the Marquesas Islands where, during the embalming process, the crushed fruits of *Fagraea berteroana* were rubbed on cadavers head to prevent hair from shedding [7].

Fagraea berteroana A.Gray ex Benth. (Gentianaceae), sometimes wrongly spelled *Fagraea berteriana*, is a tree of moderate height, naturally distributed throughout the South Pacific, except for Hawaii where it has been introduced. It is known under several names such as *pualulu* in Samoa, *pua kenikeni* in Hawaii, *pua 'enana* or *ka'upe* in the Marquesas Islands [3], or simply *pua* in Tahiti [8]. It produces fragrant tubular white flowers that later turn yellow and seasonally yield 5 cm-long and ellipsoid, orange fruits [9] (Figure 1).

A study focused on the potential of the flowers in the fragrance industry revealed volatile compounds benzyl acetate, methyl benzoate, benzyl benzoate, myristic acid, benzyl salicylate, (E)-β-ocimene, methyl salicylate, acetoin, acetic acid, nerolidol, and heneicosane as main components of the essential oil and flower headspace [10]. The fragrant flowers are traditionally well known throughout Polynesia. In Hawaii, they are used to make ceremonial leis, while in French Polynesia they are macerated in coconut oil to obtain scented monoi [11,12]. Thus, further demonstrating the importance of *F. berteroana* in Polynesian cosmetopoeia.

Literature shows that little is known concerning the chemical composition of this species or its biological activities. Studies on other species of the genus *Fagraea* revealed diverse compound families such as alkaloids, secoiridoid glycosides, coumarins, flavanols, other phenols, and lignans in the stem bark, roots, and leaves [13–21]. The only chemistry-related study on the fruits is of *F. fragrans* Roxb. (now named *Cyrtophyllum fragrans* (Roxb.) DC.) and focused on the amidation of ursolic and oleanolic acids, two components naturally present in this plant part [22].

The peculiar ethnobotanical use specific to the Marquesan Islands and the lack of phytochemistry studies on this plant made it an interesting candidate for research into its hair growth activity through modulation of the hair cycle. The latter consists of three periodic phases, the anagen phase during which the hair elongates, the catagen phase when the epithelial cells of the hair undergo apoptosis, and telogen phase when the hair rests then sheds [23,24]. Several pathways have been reported to intervene during the hair cycle, namely Wnt/β-catenin, Sonic hedgehog (Shh), Transforming Growth Factor beta (TGFB), Phosphoinositide 3-kinase PI3K/AKT, Bone Morphogenetic Protein (BMP), and Fibroblast Growth Factor (FGF) [24–28]. Among these, Wnt, TGFB, and BMP are most discussed during the telogen-to-anagen and anagen-to-catagen transitions, for their role in signaling interactions between mesenchymal and epithelial cells [24]. Activation of the canonical Wnt pathway is essential for transitioning to and maintaining the anagen

phase [26]. BMPs [29] and TGFβs [25] are paracrine effectors of the dermal papilla cells that target epithelial cells and promote the telogen and catagen phases, respectively.

In this study, we focused on Cyclin-D1 (*CCND1*) a downstream gene target of the Wnt pathway and its crucial regulatory protein, β-catenin [30]. We also assessed Bone Morphogenetic Protein 2 (*BMP2*) and Transforming growth factor beta 1 (*TGFB1*) levels.

We hypothesized that the extract and fractions would stimulate hair dermal papilla cell induction via regulation of the studied factors of the Wnt, TGFB, and BMP pathways. This would suppose a potential promotion of the anagen phase. To do so, cell proliferation activity of the ethyl acetate extract of the fruits of *F. berteroana* (FEAE) including its four resulting fractions FEAE-F0, FEAE-F1, FEAE-F2, FEAE-F3 of differing polarity obtained after open column fractioning was determined by 3-(4,5-dimethylthiazol-2-yl)-2,5-diphenyltetrazolium bromide (MTT) assay on hair follicle dermal papilla cells. RT-qPCR was performed to select the most active fraction according to its regulation of the three gene targets of the hair cycle. FEAE-F0 was thus selected and subjected to immunostaining to follow its regulation of β-catenin protein. Finally, UHPLC-ESI-MS/MS analysis of FEAE-F0 was performed to tentatively assess its chemical composition. These results are the first cellular assays focused on *F. berteroana* fractions and extracts.

2. Materials and Methods

2.1. Plant Material Collection, Extraction, and Fractionation

The fruits of *F. berteroana* A. Gray ex Benth. were collected in April 2018 in Tahiti (17°34.646′ S 149°36.363′ W), French Polynesia. The tree was identified by the botanist Jean-François Butaud. A voucher specimen (K HUGHES 4) was deposited at the herbarium of French Polynesia (PAP). The fruits were oven-dried at 40 °C for 2 days then ground to a 2 mm powder. The powder was macerated in ethyl acetate during 12 h, under agitation. The liquid ethyl acetate extract was evaporated until a viscous extract was obtained. The ethyl acetate *F. berteroana* extract (FEAE) was further fractioned (10.89 g) using open column chromatography with silica gel 60 Å. The solvents chosen were cyclohexane, ethyl acetate (EtOAc), and methanol in a gradually polar system. The elution started with two column volumes of cyclohexane/EtOAc (80/20) followed by one column volume of cyclohexane/EtOAc (60/40) which led to the first fraction FEAE-F0. The second fraction FEAE-F1 was obtained by recovering the 2nd volume of cyclohexane/EtOAc (60/40) and the first volume of cyclohexane/EtOAc (70/30). FEAE-F2 is composed of the 2nd volume of cyclohexane/EtOAc (70/30) and 100% EtOAc, and finally, FEAE-F3 is the fraction eluted with 100% methanol. All fractions were evaporated till dry. A fraction of the dried fractions was later dissolved in dimethylsufoxide (DMSO) to obtain a 1% solution for the cellular assays.

2.2. Cell Viability via the MTT Assay

Human hair follicle dermal papilla cells (HDPCs) were purchased from Promocell (Heidelberg, Germany) and grown in follicle dermal papilla cell growth medium (Promocell, Sickingenstr, Heidelberg, Germany) supplemented with 100 $U \cdot mL^{-1}$ penicillin and 100 $\mu g \cdot mL^{-1}$ streptomycin (Gibco). The cells were cultured in a humidified atmosphere at 37 °C and 5% CO_2. The Cell Proliferation kit I MTT assay (Roche, Manheim, Germany) was performed to assess the influence of the extracts on the viability of HDPCs. Cells were seeded (10^4 and 8×10^3 for 24- and 48-h experiments, respectively) into 96-well plates. They were treated with 200 µL of increasing concentrations of the extracts, ranging from 0.1 $\mu g \cdot mL^{-1}$ to 50 $\mu g \cdot mL^{-1}$. The control group consisted of DMSO diluted in medium to concentrations ranging from 0.001% to 0.5%, similarly to those of the extracts. The plates were incubated at 37 °C and 5% CO_2 for 24 h and 48 h independently. The supernatant was then discarded and 100 µL of 10% MTT in fresh medium was added to the wells and incubated for 4 h before adding 100 µL of solubilization solution. The plates were incubated overnight, and the absorbance was read on a Multiskan GO spectrophotometer (Thermoscientific, Inc., Vantaa, Finland) at 570 and 690 nm. All tests were done at least

in triplicate. The absorbance of each extract concentration was normalized to its corresponding control. Statistical analyses were performed on results as described in Section 2.5 Statistical analysis.

2.3. Quantitative Real-Time Polymerase Chain Reaction (qRT-PCR)

Cells were seeded in 6-well plates and treated with DMSO 0.5% in medium or the extracts diluted in medium. Total RNA was extracted from cells using TRIzol® reagent (Thermo Fisher Scientific, Inc., Carlsbad, CA, USA). After quantification on a Nanodrop 1000 spectrophotometer (Thermo Fisher Scientific, Inc., Wilmington, DE, USA), 750 ng of RNA were reversed transcribed to cDNA with Superscript IV (ThermoFisher Scientific, Inc., Vilnius, Lithuania). The qRT-PCR was performed to detect the expression of genes of interest using SYBR-Green PCR Master Mix (Roche, Mannheim, Germany) with a Lightcycler 480 II Roche system (Roche, Manheim, Germany). The thermocycling conditions were as follows: initial denaturation at 95 °C for 2 min, then denaturation at 95 °C for 15 s, annealing at 56 °C for 15 s and extension at 68 °C for 20 s, for a total of 40 cycles. The gene expression was normalized to Calmodulin 2 (CALM2), Glyceraldehyde 3-phosphate dehydrogenase (GAPDH), and Pumilio homolog 1 (PUM1) expressions. The expression level of the genes of interest was calculated using the $2^{-\Delta\Delta Cq}$ method. Primers were designed and obtained from Eurogentec (Table 1). The expression level obtained after the $2^{-\Delta\Delta Cq}$ of each treatment for a given gene was finally normalized to the replicate mean of its corresponding DMSO control. Statistical analyses were performed on gene expression values as described in Section 2.5 Statistical analysis.

Table 1. List of designed primer sequences used for qRT-PCR analysis.

Gene Names	Forward Primer	Reverse Primer
BMP2	5′-CCC-ACT-TGG-AGG-AGA-AAC-AA-3′	5′-GCT-GTT-TGT-GTT-TGG-CTT-GA-3′
CALM2	5′-GGG-AAC-ATC-TGG-GTT-ATG-CC-3′	5′-GAC-TGT-CCA-TAG-TCC-ACG-CA-3′
CCND1	5′-AAC-TAC-CTG-GAC-CGC-TTC-CT-3′	5′-CCA-CTT-GAG-CTT-GTT-CAC-CA-3′
GAPDH	5′-CCA-GCA-AGA-GCA-CAA-GAG-GA-3′	5′-TGG-TTG-AGC-ACA-GGG-TAC-TT-3′
PUM1	5′-GGT-GCC-CTT-GTA-GTG-AAT-GC-3′	5′-TGT-TGT-TCC-AGC-AAG-ACC-AC-3′
TGFB1	5′-CTG-GCG-ATA-CCT-CAG-CAA-CC-3′	5′-CGG-TAG-TGA-ACC-CGT-TGA-TGT-C-3′

2.4. Direct Immunofluorescence Staining

The cells were seeded on 24-well plates (Corning, Durham, NC, USA) and treated with either medium alone or FEAE-F0 for 72 h. The HDPCs were then fixed with 4% paraformaldehyde (Thermoscientific, Rockford, IL, USA) during 15 min at room temperature, then permeabilized with Triton 0.1X and saturated for 30 min in 10% fetal bovine serum (FBS). The cells were then directly stained with mouse β-catenin antibody (1:25) conjugated with AlexaFluor 488 (Santa Cruz, Dallas, TX, USA) in 1% FBS overnight at 4 °C.

The nuclei were counterstained with Hoechst 33342 Solution (Thermoscientific, Illinois, USA) the following day. The images were obtained immediately after counterstaining on the microscope AxioObserver 7 (Zeiss, Jena, Germany) and analyzed with the software Fiji coupled to ImageJ version 2.0. According to the protocol set by The University of Queensland [31] with slight modifications.

The analysis of the images obtained from the microscope was carried out as follows.

The surface of each cell nuclei was selected via a macro command on the image obtained for the β-catenin green fluorescence. The selected regions were measured for the area and integrated density (ID). All selections with an area below 640 were discarded as these did not correspond to cells but specks of fluorescence or other artefacts. A mean background value (MBGV) was also measured by selecting a dark region with no cells. The corrected total cell fluorescence (CTCF) was obtained using Equation (1).

$$\text{CTCF} = \text{ID of specific cell} - (\text{Area of cell} \times \text{MBGV}) \quad (1)$$

The same steps were also done in blue fluorescence for the same cells selected in the green channel. A normalized CTCF value was obtained by dividing the CTCF obtained for the green channel of each cell to the corresponding CTCF in the blue channel. The results obtained were averaged to obtain a mean normalized CTCF equated to nuclear β-catenin expression levels.

2.5. Statistical Analysis

Data on cell-based tests were expressed as mean ± SE (standard error) of at least three independent experiments. The statistical tests were performed on Stata14. A *F*-test was performed to determine equality of the variances between the control group mean and each treatment group mean, followed by an unpaired Student's *t*-test. Welch's *t*-test was performed if variances were unequal. A p-value ≤ 0.05 was considered significant.

2.6. UHPLC-MS/MS Analysis of F. berteroana Fraction FEAE-F0

The chemical analyses were performed on a UHPLC system (Dionex Ultimate 3000, Thermo Scientific® equipped with a photodiode array detector: 254, 280, 340, and 450 nm) coupled to a high-resolution mass spectrometer (HRMS QqToF Impact II equipped with an electrospray ionization source, Bruker Daltonics, Germany) in positive and negative ionization modes (20 eV and 40 eV). The extracts were prepared by solubilizing 1 mg of dry extract in 1 mL of methanol then filtered with a 0.2 µm syringe filter. The separations were carried out on an Acclaim RSLC C18 column (2.1 mm × 150 mm, 2.2 µm, DIONEX Thermo Scientific®, Sunnyvale, CA, USA) at 40 °C by injecting 2 µL of the prepared solution.

The chromatographic analytical method was developed to obtain the best chromatographic separation, with H_2O + 0.1% formic acid (solvent A) and acetonitrile + 0.1% formic acid (solvent B). The program consisted of 2 min at 5% B followed by a linear gradient up to 100% B for 8 min, then 100% B for 3 min and ended by a 3 min re-equilibration at 5% B (same flow rate). The injection of a formate acetate solution in basic media forming clusters on the studied mass range was used for mass calibration before each analysis.

Mass spectra were acquired ranging from 50 to 1200 m/z at 2Hz. The nebulizer pressure was set at 50.8 psi, the capillary voltage at 3000 V, the dry gas flow rate at 12 $L{\cdot}min^{-1,}$ and dry temperature at 200 °C.

The MS/MS spectral data obtained were compared to entries in repositories such as MassBank of North America [32] and MassBank [33], the METlin library, and literature data when available (Table S1).

3. Results and Discussion

3.1. Hair Follicle Dermal Papilla Cells (HDPCs) Proliferation Dynamic after Treatment with Extracts and Target Genes Regulation

The HDPCs were treated with the extracts during both 24 and 48 h to study cell viability and proliferation dynamics as seen in Figure 2A–E.

After 24 h of treatment, FEAE and FEAE-F0 induced a dose-dependent proliferation of HDPCs (Figure 2A,E). It resulted in the highest cell proliferation after 24 h of treatment at 50 $\mu g{\cdot}mL^{-1}$ amongst all the other fractions, with a 1.43-fold increase compared to the control. FEAE-F1 and FEAE-F2, also stimulated cell proliferation compared to the control after 24 h of treatment between 6.25 and 25 $\mu g{\cdot}mL^{-1}$, although not dose-dependent. FEAE-F3 also promoted cell proliferation in cells between 12.5 and 50 $\mu g{\cdot}mL^{-1}$. Furthermore, after 48 h of treatment, FEAE-F0 also induced a dose-dependent proliferation of HDPCs, along with FEAE-F3. FEAE-F3 induced a 1.24-fold increase in cell proliferation compared to the control. On the other hand, FEAE showed no significant effect on cell proliferation after 48 h of treatment.

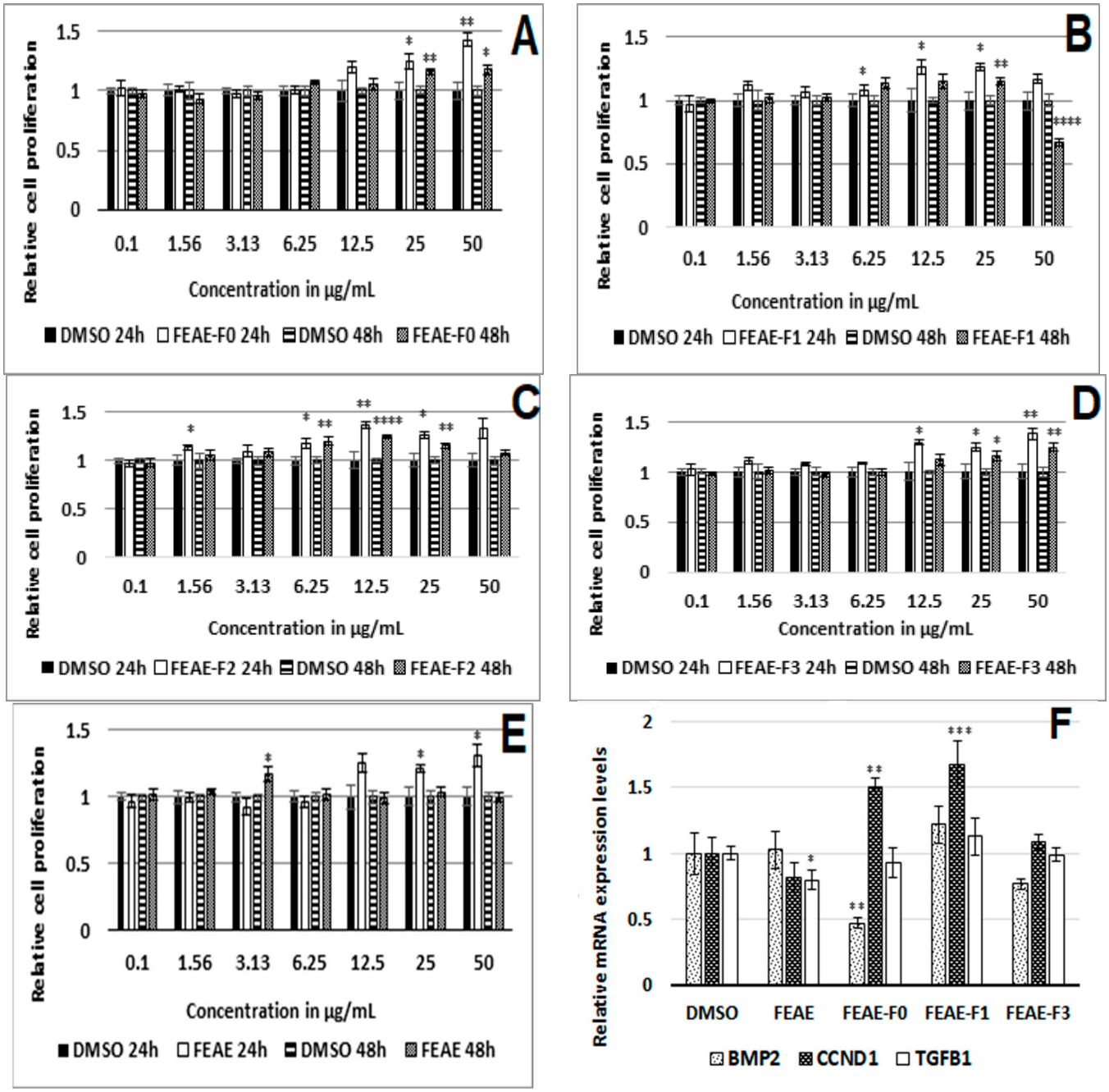

Figure 2. Relative cell proliferation activity after 24 h and 48 h treatment with FEAE-F0 (**A**), FEAE-F1 (**B**), FEAE-F2 (**C**), FEAE-F3 (**D**), FEAE (**E**) and the extracts mRNA regulation of bone morphogenetic protein 2 (*BMP2*), cyclin-D1 (*CCND1*) and transforming growth factor beta (*TGFB1*) ± S.E. (**F**). Significance is determined by ‡ $p < 0.05$, ‡‡ $p < 0.01$, ‡‡‡ $p < 0.001$ and ‡‡‡‡ $p < 0.0001$.

The RNA experiments were conducted by treating the cells with FEAE, FEAE-F0, and FEAE-F3 at 50 µg·mL^{-1}, FEAE-F1 at 25 µg·mL^{-1} and the 0.5% DMSO control during 48 h, according to the results of the cell proliferation assay. Further testing on FEAE-F2 at 25 µg·mL^{-1} was excluded because we observed a persistent adverse effect on the physiological state of the cells when seeded in 6-well plates. Three gene targets were studied, Cyclin D1 *(CCND1)*, Transforming growth factor beta 1 (*TGFB1*), and Bone Morphogenetic Protein 2 (*BMP2*) (Figure 2F). BMP2 is an inhibitor of the anagen, thus follicle growth, phase. Its levels are highest during the refractory telogen phase and rapidly decrease to allow entry into a new anagen phase [22]. Similarly, TGFB1 is a paracrine effector that facil-

itates catagen entry while Wnt activation decreases [25,34]. The extract FEAE significantly decreased *TGFB1* expression 1.22-fold ($p = 0.04$) when compared to the control using a Student *t*-test. This modulation of the *TGFB1* gene expression was not found in any of the fractions. Nonetheless, FEAE-F0 induced a significant 2-fold ($p = 0.005$) decrease of *BMP2* while simultaneously increasing *CCND1* 1.5-fold ($p = 0.002$). FEAE-F1 also enabled a significant 1.7-fold ($p = 0.007$) increase in *CCND1* but had no significant effect on the expression levels of *BMP2*. FEAE-F3 showed no significant regulation of any of the studied genes.

Reported studies have shown crosstalk between Wnt and TGFβ signaling [35,36]. Inhibitors of the Wnt pathway show a subsequent increase in TGFβ signaling in non-balding cells, as well as an increased TGFβ1 expression [36]. Likewise, BMP signaling prohibits activation of the Wnt pathway during the telogen phase. As the signaling environment of the cells changes, BMP levels lower to allow an upregulation of Wnt signaling and thus entry into anagen phase [24]. FEAE-F0 stood out as the most active fraction by displaying a similar regulation. Indeed, it not only increased activation of the Wnt pathway, as seen by the upregulation of *CCND1*, but it also downregulated *BMP2*. By lowering BMP signaling, FEAE-F0 facilitates transitioning to the follicle growth (anagen) phase. This can be observed by an increase in Wnt signaling [24]. *CCND1* is a downstream target of the Wnt pathway and a rise in its expression levels suggested a stimulated Wnt state that we aimed to confirm by following β-catenin expression in the presence of FEAE-F0.

3.2. Modulation of β-Catenin Production by FEAE-F0

As β-catenin is a key protein of the Wnt pathway that intervenes during the growth phase of hair follicles [37], the effect of FEAE-F0 on its expression was studied (Figure 3). Indeed, when the Wnt/β-catenin pathway is inactive, β-catenin in the cytoplasm is phosphorylated by a complex composed of glycogen synthase kinase 3β, Axin, Adenomatous polyposis coli, and casein kinase 1a. The phosphorylated β-catenin is then ubiquitinated and recognized by a proteasome that degrades it before it enters the nucleus [38,39]. Conversely, when the canonical Wnt pathway is activated, the phosphorylating complex is inhibited which allows β-catenin to stabilize, accumulate in the cytoplasm, and successfully translocate to the nucleus [30]. Once in the nucleus, β-catenin serves as a co-activator of several downstream targets such as cyclin-D1 [40]. According to our experiments in Figure 3, FEAE-F0 showed a significant ($p < 0.0001$) 1.34-fold increase of nuclear β-catenin after treatment of HDPCs for 72 h compared to the control. Increased β-catenin levels in the nucleus are indicative of an active Wnt state allowing signaling to downstream targets [37]. Furthermore, it is important to note that this effect is done in a controlled manner. Indeed, while activation of the Wnt pathway in hair follicle cells is paramount for induction of the anagen phase and *in fine* hair growth, overexpression of the Wnt pathway could lead to developing cancerous cells [41]. FEAE-F0 showed a controlled proliferation and upregulation of the Wnt pathway which further crystallizes its efficiency in promoting hair growth.

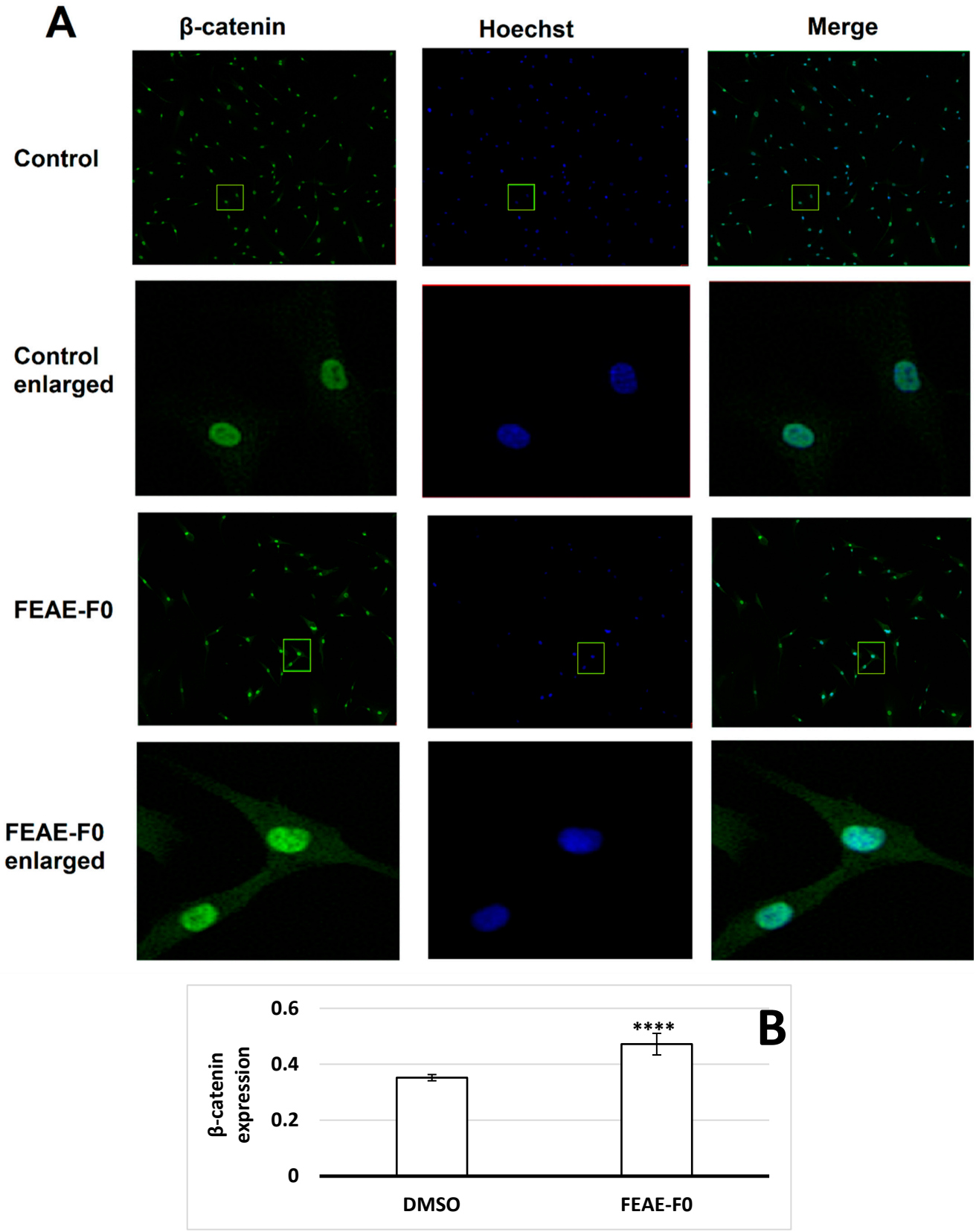

Figure 3. (**A**) β-catenin expression in dermal papilla cells after 72 h of treatment in control medium or supplemented in 50 µg·mL^{-1} FEAE-F0 and nuclei counterstained with Hoechst followed by immunofluorescence. Objective ×10 and enlarged images ×4. Green rectangles correspond to zoomed area. (**B**) Relative nuclear β-catenin expression levels in immunocytochemistry (ICC) after 72 h growth in medium with 0.5% DMSO or FEAE-F0 at a concentration of 50 µg·mL^{-1}. Significance is determined by **** $p < 0.0001$.

3.3. Chemical Composition of F. berteroana FEAE-F0

An identification of the main compounds present in FEAE-F0 was attempted by UHPLC-MS/MS analysis. The MS/MS data analyzed was that of 20 eV and 40 eV collision energy in positive and negative ionization mode. Thirteen main peaks were identified on the UV chromatogram in Figure 4. The compilation and tentative identification of the peaks by MS^2 correspondence were reported in Table 2.

Our previous work on FEAE revealed the presence of loganic and coumaric acids [42]. The present paper mainly focused on the minor bioactive fraction FEAE-F0, derived from FEAE the crude extract previously studied [42]. An exhaustive search of all compounds found in the literature for the genus *Fagraea* and their available MS^2 was compiled in Table S1 (Supplementary Material). We compared the obtained data for the thirteen peaks to that of Table S1. Only one iridoid was successfully annotated, boonein. Indeed, boonein and several other iridoids such as (±)-gentiolactone, naucledal, angelone, swermacrolactone C amongst others (Table S1) were found in the stem bark of *F. fragrans* (syn. of *Cyrtophyllum fragrans*) [17,19,20,43]. No biological activities linked to hair care have been specified for boonein in literature. Nevertheless, iridoids are known for their anti-inflammatory and cardiovascular activity [44,45]. This could suggest an implication in hair growth by enabling proper vascularization and thus maintaining nutrient support for the efficient proliferation of dermal papilla cells, notably during the anagen phase [46]. Indeed, minoxidil, one of the only FDA-approved treatments to promote hair growth, is known to mediate its effects via different mechanisms such as promoting vascularization around HDPCs [47]. Moreover, minoxidil has been reported to prolong anagen in hair follicles [26,48].

Overall, the remaining compounds that have not yet been identified, showed carbon atoms ranging between 9 and 16, suggesting medium-sized molecules. Their molecular formulas led to many structural propositions amongst known compounds in Pubchem (Table 2), thus uncovering a plethora of structural possibilities.

A few structural hypotheses could nevertheless be proposed.

According to mass and molecular formulas, FEAE-F0 included several isomers. Compounds 6 (m/z = 181.1223) and 11 (m/z = 181.1224), as well as compounds 4 (m/z = 213.1454) and 8 (m/z = 213.1484) only differed in fragmentation pattern. The MS^2 experimental data at 20 eV for compound 90552 in Metlin is remarkably similar to that of compound 6; the 40 eV spectrum fragmentation did not match as closely. Entry 90552 in Metlin corresponds to dihydroactinidiolide (DHA), which raises the hypothesis of the potential presence of DHA in our fraction, or of closely related terpenoid structures. Such a proposition may be plausible as DHA is a terpene obtained by cleavage of β-carotene [49]. As previously stated, the fruits of *F. berteroana* are reddish-orange when ripe. This latter point could explain a putative presence of β-carotene derivatives in our fraction. However, compound 11 had less fragments that matched with compound 90552. It could potentially correspond to an isomer of DHA. The resulting fragments of compound 11 could suggest either a linear structure with the loss of oxygen or a substituted phenyl ring (m/z = 91), followed by a successive loss of carbon atoms. Such a pattern could potentially correspond to shorter chained derivatives of the diterpene phytol, or potentially terpenoids containing an aromatic ring core. Interestingly, several terpenes have been the object of patents for their efficiency in preventing hair loss and promoting hair growth [50,51]. Nevertheless, the above propositions remain hypotheses.

Table 2. Corresponding MS data compilation of peaks present in FEAE-F0 chromatogram.

		Positive Mode			Negative Mode		UV (nm)	Database Search (21/01/2021)			
Peak No.	**Rt (min)**	**$[M + H]^+$**	**$[M + Na]^+$**	**Product Ions (MS/MS, 20 and 40 eV)**	**$[M - H]^-$**	**Product Ions (MS/MS)**		**Metlin**	**MetFrag (vs. Pubchem)**	**Molecular Formula**	**Compound Annotation**
1	7.67	171.1019	193.084	20 eV: 57 (100, $C_4H_9^+$), 83 (10, $C_5H_7O^+$), 111 (19, $C_7H_{11}O^+$), 125 (4, $C_8H_{13}O^+$) 40 eV: 55 (21, $C_4H_7^+$), 57 (100, $C_4H_9^+$), 59 (10, $C_3H_7O^+$), 97 (17, -), 145 (10, -)	-	-	224	3 entries, no experimental MS^2 spectra	5240 candidates	$C_9H_{14}O_3$	boonein
2	7.82	181.0861	203.0681	20 eV: 57 (100, $C_3H_5O^+$), 117 (6, $C_9H_9^+$), 131 (4, -), 151 (3, $C_8H_7O_3^+$) 40 eV: 57 (100, $C_3H_5O^+$), 91 (57, $C_7H_7^+$), 109 (36, -), 115 (50, $C_9H_7^+$), 127 (21, -), 152 (20, -)	-	-	225, 274	21 entries, 7 experimental MS^2 spectra, no correspondence	3909 candidates	$C_{10}H_{12}O_3$	-
3	8.22	153.0915	175.0734	20 eV: 67 (46, $C_5H_7^+$), 79 (85, $C_6H_7^+$), 91 (74, $C_7H_7^+$), 105 (25, $C_8H_9^+$), 107 (100, $C_8H_{11}^+$) 40 eV: 53 (28, $C_4H_5^+$), 55 (22, $C_4H_7^+$), 65 (71, $C_5H_5^+$), 67 (27, $C_5H_7^+$), 79 (44, $C_6H_7^+$), 91 (100, $C_7H_7^+$)	-	-	226, 279	13 entries, 2 experimental MS^2 spectra, no correspondence	3668 candidates	$C_9H_{12}O_2$	-
4	8.57	213.1454	-	20 eV: - 40 eV: 55 (39, $C_4H_7^+$), 57 (28, -), 91 (67, -), 91 (64, $C_7H_7^+$), 95 (41, $C_6H_7O^+$), 145 (100, -)	-	-	226, 279	13 entries, 2 experimental MS^2 spectra, no correspondence	4703 candidates	$C_{12}H_{20}O_3$	-
5	8.83	-	-	-	-	-	226, 279			-	-
6	9.00	181.1223	203.1044	20 eV: 79 (21, $C_6H_7^+$), 81 (29, $C_6H_9^+$), 93 (64, $C_7H_9^+$), 95 (56, $C_7H_{11}^+$), 107 (93, $C_8H_{11}^+$), 121 (42, $C_9H_{13}^+$), 135 (84, $C_{10}H_{15}^+$), 145 (22, $C_{11}H_{13}^+$), 163 (58, $C_{11}H_{15}O^+$), 181 (100, $C_{11}H_{17}O_2^+$) 40 eV: 53 (33, $C_4H_5^+$), 55 (40, $C_4H_7^+$), 67 (31, $C_5H_7^+$), 69 (17, $C_5H_9^+$), 79 (69, $C_6H_7^+$), 91 (100, $C_7H_7^+$), 93 (47, $C_7H_9^+$), 105 (47, $C_8H_9^+$), 107 (24, $C_8H_{11}^+$)	-	-	226, 284	12 entries, 1 experimental MS^2 spectrum hypothetical match Metlin ID 90552	6090 candidates	$C_{11}H_{16}O_2$	-
7	9.36	-	-	-	217.0874	20 eV: 117.0346 (33, $C_8H_5O^-$), 119.0503 (100, $C_8H_7O^-$), 145.0296 (51, $C_9H_5O_2^-$), 163.0402 (28, $C_9H_7O_3^-$), 217.0873 (9, $C_{13}H_{13}O_3^-$) 40 eV: 89 (3, $C_7H_5^-$), 93 (5, $C_6H_5O^-$), 117 (100, $C_8H_5O^-$), 119 (38, $C_8H_7O^-$), 145 (5, $C_9H_5O_2^-$)	227	7 entries, 1 experimental MS^2 spectrum, no correspondence	5081 candidates	$C_{13}H_{14}O_3$	-
8	9.45	213.1484	235.1306	20 eV: 57 (100, $C_4H_9^+$), 81 (4, $C_6H_9^+$), 83 (5, $C_6H_{11}^+$), 109 (5, $C_7H_9O^+$), 127 (48, $C_7H_{11}O_2^+$), 139 (6, $C_8H_{11}O_2^+$), 195 (10, $C_{12}H_{19}O_2^+$) 40 eV: 57 (100, $C_4H_9^+$), 79 (8, $C_6H_7^+$), 81 (14, $C_6H_9^+$), 109 (3, $C_7H_9O^+$), 127 (8, $C_7H_{11}O_2^+$)	211.1344 (low)	-	227	13 entries, 2 experimental MS^2 spectra, no correspondence	4703 candidates	$C_{12}H_{20}O_3$	-

Table 2. *Cont.*

		Positive Mode			Negative Mode		UV (nm)	Database Search (21/01/2021)			
Peak No.	**Rt (min)**	**$[M + H]^+$**	**$[M + Na]^+$**	**Product Ions (MS/MS, 20 and 40 eV)**	**$[M - H]^-$**	**Product Ions (MS/MS)**		**Metlin**	**MetFrag (vs. Pubchem)**	**Molecular Formula**	**Compound Annotation**
9	9.52	223.0965	247.0745	20 eV: 121 (2, $C_7H_5O_2^+$), 149 (100, $C_8H_5O_3^+$), 177 (7, $C_{10}H_9O_3^+$) 40 eV: 65 (80, $C_5H_5^+$), 93 (19, $C_6H_5O^+$), 111 (10, $C_6H_7O_2^+$), 121 (72, $C_7H_5O_2^+$), 149 (100, $C_8H_5O_3^+$), 167 (4, $C_8H_7O_4^+$)	-	-	228, 277	13 entries, 1 experimental MS^2 spectrum, no correspondence	6105 candidates	$C_{12}H_{14}O_4$	-
10	9.80	-	-	-	195.1393	20 eV: 109 (8, $C_7H_9O^-$), 111 (6, $C_7H_{11}O^-$), 125 (3, $C_8H_{13}O^-$), 138 (12, $C_8H_{10}O_2{}^-$), 167 (16, $C_{11}H_{19}O^-$), 179 (24, $C_{11}H_{15}O_2{}^-$), 195 (100, $C_{12}H_{19}O_2{}^-$) 40 eV: 53 (100, C_3HO^-), 109 (11, $C_7H_9O^-$), 122 (14, $C_7H_6O_2{}^-$), 138 (14, $C_8H_{10}O_2{}^-$)	227	59 entries, 1 experimental MS^2 spectrum, no correspondence	6334 candidates	$C_{12}H_{20}O_2$	-
11	10.50	181.1224	203.1045	20 eV: 93 (53, $C_7H_9^+$), 95 (28, $C_6H_7O^+$), 97 (25, $C_6H_9O^+$), 107 (32, $C_8H_{11}^+$), 111 (17, $C_7H_{11}O^+$), 125 (100, $C_7H_9O_2^+$), 135 (37, $C_{10}H_{15}^+$), 138 (22, $C_8H_{10}O_2^+$), 163 (28, $C_{11}H_{15}O^+$), 181 (94, $C_{11}H_{17}O_2^+$) 40 eV: 53 (50, $C_4H_5^+$), 55 (40, $C_4H_7^+$), 65 (20, $C_5H_5^+$), 67 (44, $C_5H_7^+$), 77 (19, $C_6H_5^+$), 79 (38, $C_6H_7^+$), 81 (12, $C_6H_9^+$), 91 (100, $C_7H_7^+$), 93 (42, $C_7H_9^+$), 95 (70, $C_6H_7O^+$), 97 (22, $C_6H_9O^+$), 105 (21, $C_8H_9^+$), 109 (20, $C_7H_9O^+$), 123 (11, $C_7H_7O_2^+$), 125 (12, $C_7H_9O_2^+$)	-	-	228, 276	12 entries, 1 experimental MS^2 spectrum no close match	6090 candidates	$C_{11}H_{16}O_2$	-
12	10.98	209.1538	231.1357	20 eV: - 40 eV: 53 (10, $C_4H_5^+$), 55 (36, $C_4H_7^+$), 57 (100, $C_4H_9^+$), 59 (30, $C_3H_7O^+$), 65 (7, $C_5H_5^+$), 67 (56, $C_5H_7^+$), 69 (15, $C_5H_9^+$), 77 (5, $C_6H_5^+$), 79 (42, $C_6H_7^+$), 81 (31, $C_6H_9^+$), 83 (4, $C_5H_7O^+$, 5, $C_6H_{11}^+$), 91 (49, $C_7H_7^+$), 93 (31, $C_7H_9^+$), 95 (9, $C_6H_7O^+$, 15, $C_7H_{11}^+$), 97 (12, $C_6H_9O^+$), 103 (6, $C_8H_7^+$), 105 (46, $C_8H_9^+$), 107 (37, $C_8H_{11}^+$), 109 (8, $C_7H_9O^+$), 111 (4, $C_7H_{11}O^+$), 119 (18, $C_9H_{11}^+$), 121 (17, $C_9H_{13}^+$), 123 (3, $C_7H_7O_2^+$, $C_8H_{11}O^+$, $C_9H_{15}^+$), 133 (10, $C_{10}H_{13}^+$), 135 (8, $C_{10}H_{15}^+$), 151 (6, $C_{10}H_{15}O^+$), 179 (11, $C_{11}H_{15}O_2^+$), 194 (4, $C_{12}H_{18}O_2^+$)	-	-	228, 292	13 entries, no experimental MS^2 spectra	6905 candidates	$C_{13}H_{20}O_2$	-
13	11.45	279.1594	301.1414	20 eV: 57 (10, $C_4H_9^+$), 109 (2, $C_8H_{13}^+$), 149 (100, $C_8H_5O_3^+$), 167 (5, $C_8H_7O_4^+$), 209 (2, $C_{10}H_9O_5^+$) 40 eV: 57 (19, $C_4H_9^+$), 121 (23, $C_7H_5O_2^+$), 149 (100, $C_8H_5O_3^+$), 167 (5, $C_8H_7O_4^+$)	-	-	227, 279	4 entries, 1 experimental MS^2 spectrum, no correspondence	5392 candidates	$C_{16}H_{22}O_4$	-

Rt = retention time.

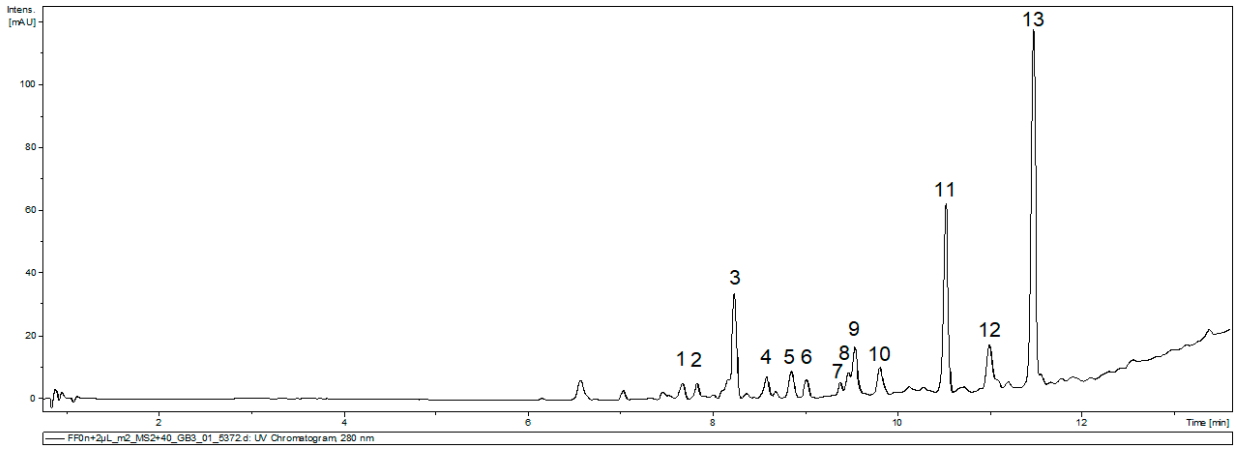

Figure 4. UV chromatogram of FEAE-F0 at 280 nm for the 40 eV positive ionization mode.

4. Conclusions

Our results showed that there is a positive correlation between the ethnocosmetic use of the fruits of *F. berteroana* and observed molecular activities. Indeed, an ethyl acetate extract of the fruits and fractions FEAE-F0 through FEAE-F3 could potentiate hair growth via stimulation of hair follicle dermal papilla cells proliferation, shown herein by in vitro induction of HDPCs. Furthermore, FEAE-F0 was selected for its potential positive effect on the anagen phase of the hair cycle by upregulating the Wnt pathway, alongside down-regulating the BMP pathway. The in vitro activity observed for FEAE-F0 can be attributed to its chemical content, comprising of iridoids and potentially terpenoids. The fraction stands out as an interesting natural active for applications in hair growth. This could further be cemented with *in* and ex vivo studies geared towards the prevention of hair loss due to genetic factors such as androgenetic alopecia, or environmental stresses.

Lastly, the actual natural resource is limited in low- to mid-altitude in French Polynesia, but its cultivation is not unreasonable as the tree is often grown in marae, a large and clear area devoted to traditional or communal practices in Polynesian societies, because of its spiritual symbolism or gardens. Hence, an effort to cultivate it could be successful and interesting to obtain a sustainable resource for further development of this plant material as a potential natural cosmetic ingredient.

Supplementary Materials: The following are available online at https://www.mdpi.com/2079-9284/8/1/13/s1, Table S1: MS2 data compilation of the compounds present in the *Fagraea* genus according to literature.

Author Contributions: P.R., J.-Y.B., R.H., E.F. and K.H. participated in the conceptualization and general methodology design of the project and article. K.H. designed and performed the experiments, ran the data analysis, and wrote the original draft of the article. E.R. supervised fractioning of plant material. C.C. and S.H. supervised experiments in cellular biology and provided expertise for data interpretation and validation of related experiments. S.G. supervised experiments in metabolomics and provided expertise for data interpretation. J.-F.B. provided expertise in ethnobotany and in plant collection and identification. P.R., R.H., and J.-Y.B. acquired funding for the project. All authors participated in the reviewing and editing process of the article. All authors have read and agreed to the published version of the manuscript.

Funding: This research was funded by the French Ministry of Higher Education and Research at the University of French Polynesia (ED 469) and Greentech.

Institutional Review Board Statement: Not applicable.

Informed Consent Statement: Not applicable.

Acknowledgments: The authors wish to acknowledge Cosmetic Valley for their financial support. UHPLC-MS/MS was performed on the Mallabar platform (granted by Provence Alpes Côte d'Azur region, ANR and Total Foundation) at IMBE. Immunofluorescence was performed on the Anipath platform (granted by Cancéropôle Lyon Auvergne Rhône Alpes 2007 and CPER 2016). The authors would also like to thank Nicolas Allègre for his expertise in molecular analysis and Pierre Pouchin for his expertise in imagery analysis. The authors wish to warmly thank Marianne, Tohei and Tuihau Theophilus for their kind contribution to the photograph in Figure 1A.

Conflicts of Interest: The authors declare no conflict of interest. The funders had no role in the design of the study, in the collection, analyses, or interpretation of data.

References

1. Butaud, J.-F. *Synthèse Bibliographique Portant Sur Les Plantes Utilisées Dans La Cosmétopée de Polynésie Française*; Cosmetic Valley: Chartres, France, 2013.
2. Ansel, J.-L.; Ly, Q.; Butaud, J.-F.; Nicolas, M.; Herbette, G.; Peno-Mazzarino, L.; Lati, E.; Raharivelomanana, P. Activité anti-âge de l'extrait de Fitchia nutans, un ingrédient cosméticeutique d'un monoï traditionnel polynésien. *Comptes Rendus Chim.* **2016**, *19*, 1049–1055. [CrossRef]
3. Jost, X.; Ansel, J.-L.; Lecellier, G.; Raharivelomanana, P.; Butaud, J.-F. Ethnobotanical Survey of Cosmetic Plants Used in Marquesas Islands (French Polynesia). *J. Ethnobiol. Ethnomed.* **2016**, *12*. [CrossRef]
4. Martin, A. The Enlightenment in Paradise: Bougainville, Tahiti, and the Duty of Desire. *Eighteenth Century Stud.* **2007**, *41*, 203–216. [CrossRef]
5. Gauthier, L. *TAHITI—1904-1921*; Les éditions du Pacifique: Paris, France, 1985.
6. Hughes, K.; Ho, R.; Butaud, J.-F.; Filaire, E.; Ranouille, E.; Berthon, J.-Y.; Raharivelomanana, P. A Selection of Eleven Plants Used as Traditional Polynesian Cosmetics and Their Development Potential as Anti-Aging Ingredients, Hair Growth Promoters and Whitening Products. *J. Ethnopharmacol.* **2019**, *245*, 112159. [CrossRef] [PubMed]
7. Handy, E.S.C. *The Native Culture in the Marquesas*; Bernice P. Bishop Museum: Honolulu, HI, USA, 1923.
8. Pétard, P. *Plantes Utiles de Polynésie Française et Raau Tahiti*; Editions Haere Po No Tahiti: Papeete, French Polynesia, 1986; ISBN 978-2-904171-06-2.
9. Whistler, W.A.; Elevitch, C.R. *Fagraea berteroana (Pua kenikeni), Ver. 3.2.*; Volume Species Profiles for Pacific Island Agroforestry; Elevitch, C.R., Ed.; Permanent Agriculture Resources (PAR): Honolulu, HI, USA, 2006.
10. Hayashi, S.; Kameoka, H.; Hashimoto, S.; Furukawa, K.; Arai, T. Volatile Compounds of *Fagraea berteriana* Flowers. *J. Essent. Oil Res.* **1995**, *7*, 505–510. [CrossRef]
11. Whistler, W.A. *Plants in Samoan Culture: The Ethnobotany of Samoa*; Isle Botanica: Honolulu, HI, USA, 2000; ISBN 978-0-9645426-6-2.
12. Motley, T.J. The Ethnobotany of *Fagraea* Thunb. (Gentianaceae): The Timber of Malesia and the Scent of Polynesia. *Econ. Bot.* **2004**, *58*, 396–409. [CrossRef]
13. Cuendet, M.; Hostettmann, K.; Potterat, O.; Dyatmiko, W. Iridoid Glucosides with Free Radical Scavenging Properties from *Fagraea blumei*. *Helv. Chim. Acta* **1997**, *80*, 1144–1152. [CrossRef]
14. Cambie, R.C.; Lal, A.R.; Rickard, C.E.F.; Tanaka, N. Chemistry of Fijian Plants. V.: Constituents of *Fagraea gracilipes* A. GRAY. *Chem. Pharm. Bull.* **1990**, *38*, 1857–1861. [CrossRef]
15. Ferdinal, N.; Alfajri, R.; Arifin, B. Isolation and Characterization of Scopoletin from The Bark of *Fagraea ceilanica* Thumb and Antioxidants Tests. *Int. J. Adv. Sci. Eng. Inf. Technol.* **2015**, *5*, 126. [CrossRef]
16. Bangprapai, A.; Thongphasuk, P.; Songsak, T. Determination of Swertiamarin Content by Tlc-Densitometer in *Fagraea fragrans* Roxb. Leaves. *Bull. Health Sci. Technol.* **2016**, *14*, 13–18.
17. Jonville, M.-C.; Capel, M.; Frédérich, M.; Angenot, L.; Dive, G.; Faure, R.; Azas, N.; Ollivier, E. Fagraldehyde, a Secoiridoid Isolated from *Fagraea fragrans*. *J. Nat. Prod.* **2008**, *71*, 2038–2040. [CrossRef] [PubMed]
18. Okuyama, E.; Suzumura, K.; Yamazaki, M. Pharmacologically Active Components of Todopon Puok (*Fagraea racemosa*), a Medicinal Plant from Borneo. *Chem. Pharm. Bull.* **1995**, *43*, 2200–2204. [CrossRef]
19. Madmanang, S.; Cheyeng, N.; Heembenmad, S.; Mahabusarakam, W.; Saising, J.; Seeger, M.; Chusri, S.; Chakthong, S. Constituents of *Fagraea fragrans* with Antimycobacterial Activity in Combination with Erythromycin. *J. Nat. Prod.* **2016**, *79*, 767–774. [CrossRef] [PubMed]
20. Rattanaburi, S.; Kaikaew, K.; Watanapokasin, R.; Phongpaichit, S.; Mahabusarakamb, W. A New Lignan from the Stem Bark of *Fagraea fragrans* Roxb. *Nat. Prod. Res.* **2020**, 1–6. [CrossRef]
21. Wan, A.S.C.; Chow, Y.L. Alkaloids of *Fagraea fragrans* Roxb. *J. Pharm. Pharmacol.* **1964**, *16*, 484–486. [CrossRef] [PubMed]
22. Basir, D.; Hanafi, M.; Saputra, A.; Wati, T. Free Solvent Amidation of Ursolic and Oleanolic Acids of *Fagraea fragrans* Fruits: Their P-388 Antitumor Activity. *J. Phys. Conf. Ser.* **2018**, *1095*, 012006. [CrossRef]
23. Tamura, Y.; Takata, K.; Eguchi, A.; Kataoka, Y. In Vivo Monitoring of Hair Cycle Stages via Bioluminescence Imaging of Hair Follicle NG2 Cells. *Sci. Rep.* **2018**, *8*. [CrossRef]
24. Plikus, M.V. New Activators and Inhibitors in the Hair Cycle Clock: Targeting Stem Cells' State of Competence. *J. Investig. Dermatol.* **2012**, *132*, 1321–1324. [CrossRef] [PubMed]

25. Inui, S.; Itami, S. Molecular Basis of Androgenetic Alopecia: From Androgen to Paracrine Mediators through Dermal Papilla. *J. Dermatol. Sci.* **2011**, *61*, 1–6. [CrossRef] [PubMed]
26. Kwack, M.H.; Kang, B.M.; Kim, M.K.; Kim, J.C.; Sung, Y.K. Minoxidil Activates β-catenin Pathway in Human Dermal Papilla Cells: A Possible Explanation for Its Anagen Prolongation Effect. *J. Dermatol. Sci.* **2011**, *62*, 154–159. [CrossRef]
27. Zhang, H.; Su, Y.; Wang, J.; Gao, Y.; Yang, F.; Li, G.; Shi, Q. Ginsenoside Rb1 Promotes the Growth of Mink Hair Follicle via PI3K/AKT/GSK-3β Signaling Pathway. *Life Sci.* **2019**, *229*, 210–218. [CrossRef] [PubMed]
28. Dastan, M.; Najafzadeh, N.; Abedelahi, A.; Sarvi, M.; Niapour, A. Human Platelet Lysate versus Minoxidil Stimulates Hair Growth by Activating Anagen Promoting Signaling Pathways. *Biomed. Pharmacother.* **2016**, *84*, 979–986. [CrossRef]
29. Oshimori, N.; Fuchs, E. Paracrine TGF-β Signaling Counterbalances BMP-Mediated Repression in Hair Follicle Stem Cell Activation. *Cell Stem Cell* **2012**, *10*, 63–75. [CrossRef]
30. Veltri, A.; Lang, C.; Lien, W.-H. Concise Review: Wnt Signaling Pathways in Skin Development and Epidermal Stem Cells: Wnt Signaling in Skin Development and Stem Cells. *Stem Cells* **2018**, *36*, 22–35. [CrossRef] [PubMed]
31. Hammond, L. QBI, The University of Queensland Australia Measuring Cell Fluorescence Using ImageJ—The Open Lab Book v1.0. Available online: https://theolb.readthedocs.io/en/latest/imaging/measuring-cell-fluorescence-using-imagej.html (accessed on 15 October 2020).
32. MassBank of North America (MoNA)—PubChem Data Source. Available online: https://pubchem.ncbi.nlm.nih.gov/source/22043 (accessed on 20 August 2020).
33. Horai, H.; Arita, M.; Kanaya, S.; Nihei, Y.; Ikeda, T.; Suwa, K.; Ojima, Y.; Tanaka, K.; Tanaka, S.; Aoshima, K.; et al. MassBank: A Public Repository for Sharing Mass Spectral Data for Life Sciences. *J. Mass Spectrom.* **2010**, *45*, 703–714. [CrossRef] [PubMed]
34. Inui, S.; Itami, S. Androgen Actions on the Human Hair Follicle: Perspectives. *Exp. Dermatol.* **2013**, *22*, 168–171. [CrossRef]
35. Warner, D.R.; Greene, R.M.; Pisano, M.M. Cross-Talk between the TGFβ and Wnt Signaling Pathways in Murine Embryonic Maxillary Mesenchymal Cells. *FEBS Lett.* **2005**, *579*, 3539–3546. [CrossRef] [PubMed]
36. Lu, G.-Q.; Wu, Z.-B.; Chu, X.-Y.; Bi, Z.-G.; Fan, W.-X. An Investigation of Crosstalk between Wnt/β-catenin and Transforming Growth Factor-β Signaling in Androgenetic Alopecia. *Medicine* **2016**, *95*, e4297. [CrossRef] [PubMed]
37. Choi, B.Y. Targeting Wnt/β-catenin Pathway for Developing Therapies for Hair Loss. *Int. J. Mol. Sci.* **2020**, *21*, 4915. [CrossRef] [PubMed]
38. Kimelman, D.; Xu, W. β -catenin Destruction Complex: Insights and Questions from a Structural Perspective. *Oncogene* **2006**, *25*, 7482–7491. [CrossRef] [PubMed]
39. Stamos, J.L.; Weis, W.I. The β-catenin Destruction Complex. *Cold Spring Harb. Perspect. Biol.* **2013**, *5*. [CrossRef]
40. Shtutman, M.; Zhurinsky, J.; Simcha, I.; Albanese, C.; D'Amico, M.; Pestell, R.; Ben-Ze'ev, A. The Cyclin D1 Gene Is a Target of the β-catenin/LEF-1 Pathway. *Proc. Natl. Acad. Sci. USA* **1999**, *96*, 5522–5527. [CrossRef]
41. Schneider, J.A.; Logan, S.K. Revisiting the Role of Wnt/β-catenin Signaling in Prostate Cancer. *Mol. Cell. Endocrinol.* **2018**, *462*, 3–8. [CrossRef]
42. Hughes, K.; Ho, R.; Greff, S.; Filaire, E.; Ranouille, E.; Chazaud, C.; Herbette, G.; Butaud, J.-F.; Berthon, J.-Y.; Raharivelomanana, P. Hair Growth Activity of Three Plants of the Polynesian Cosmetopoeia and Their Regulatory Effect on Dermal Papilla Cells. *Molecules* **2020**, *25*, 4360. [CrossRef] [PubMed]
43. Suciati, S.; Lambert, L.K.; Ross, B.P.; Deseo, M.A.; Garson, M.J. Phytochemical Study of *Fagraea* Spp. Uncovers a New Terpene Alkaloid with Anti-Inflammatory Properties. *Aust. J. Chem.* **2011**, *64*, 489. [CrossRef]
44. Villasenor, I. Bioactivities of Iridoids. *AIAAMC* **2007**, *6*, 307–314. [CrossRef]
45. Viljoen, A.; Mncwangi, N.; Vermaak, I. Anti-Inflammatory Iridoids of Botanical Origin. *CMC* **2012**, *19*, 2104–2127. [CrossRef]
46. Li, W.; Man, X.-Y.; Li, C.-M.; Chen, J.-Q.; Zhou, J.; Cai, S.-Q.; Lu, Z.-F.; Zheng, M. VEGF Induces Proliferation of Human Hair Follicle Dermal Papilla Cells through VEGFR-2-Mediated Activation of ERK. *Exp. Cell Res.* **2012**, *318*, 1633–1640. [CrossRef] [PubMed]
47. Lachgar; Charveron; Gall; Bonafe Minoxidil Upregulates the Expression of Vascular Endothelial Growth Factor in Human Hair Dermal Papilla Cells. *Br. J. Dermatol.* **1998**, *138*, 407–411. [CrossRef]
48. Messenger, A.G.; Rundegren, J. Minoxidil: Mechanisms of Action on Hair Growth. *Br. J. Dermatol.* **2004**, *150*, 186–194. [CrossRef]
49. Shumbe, L.; Bott, R.; Havaux, M. Dihydroactinidiolide, a High Light-Induced β-Carotene Derivative That Can Regulate Gene Expression and Photoacclimation in Arabidopsis. *Mol. Plant* **2014**, *7*, 1248–1251. [CrossRef] [PubMed]
50. Marin, C.L.R. Terpene Extract for the Treatment of Hair Loss 2013. Available online: https://patentscope2.wipo.int/search/en/detail.jsf?docId=WO2013174854 (accessed on 31 January 2021).
51. Takahashi, H.; Hara, S.c/oK.K.Y.C.K.; Matsui, R.c/oK.K.Y.C.K. Diterpenes and Flavonoids as 5-Alpha-Reductase Inhibitors 1996. Available online: https://patents.google.com/patent/EP0747048A2/en (accessed on 31 January 2021).